METHODS, TOOLS and TECHNOLOGIES

Title

High density camera trap grid reveals lack of consistency in detection and capture rates across space and time

List of Authors

Joseph M. Kolowski[1†], Josephine Oley[2], William J. McShea[3]

[1] Smithsonian Conservation Biology Institute, Smithsonian-Mason School of Conservation, 1500 Remount Rd. Front Royal, VA 22630

[2]14557 Crossfield Way, Woodbridge, VA 22192

[3] Center for Conservation Ecology, Smithsonian Conservation Biology Institute, 1500 Remount Rd. Front Royal, VA 22630

†kolowskij@si.edu

Abstract

Counts of independent photo events from camera traps are commonly used to make inference about species occupancy, the density of unmarked populations, and the relative abundance of species across time and space. These applications rest on the untested assumption that data collected from individual cameras are representative of the landscape location in which they are placed, and that nearby cameras would record similar data when any additional micro-site differences are accounted for. We established a high-density camera trapping grid (100 x 100 m; 27 cameras) in Virginia, USA to explicitly test these assumptions, investigating variation in capture rates and detection probabilities for a range of terrestrial mammals during 4, 2-month seasonal surveys. Despite controlling for numerous habitat and placement factors, we documented, across all 5 focal species, large ranges and coefficients of variation in both capture rate and detection probabilities which were similar to those seen across 2 sets of independent forest sampling sites from a larger, more typical camera trap sampling design. We also documented a lack of spatial autocorrelation in capture rate at any distance. Measured local covariates relevant to the camera viewshed (stem density, camera height, log presence, effective detection distance (EDD), total dbh of oak trees) rarely explained any significant portion of observed variation in capture rates or detection probabilities across the grid. The influence of EDD, measured here for the first time for individual camera stations, was inconsistently important and varied in direction of effect depending on species and season. Our study indicates single camera stations may fail to sample animal presence and frequency of use in a robust and repeatable way, primarily resulting from the influence of both idiosyncrasies in animal movement and measured and unknown micro-site characteristics. We recommend spatial

replication within sites (e.g. small-scale shifting of cameras or use of multiple stations) should be considered to minimize impacts of relevant microsite characteristics, some of which may be difficult to identify.

Keywords

camera trap; capture rate; detection; detection bias; detection probability; imperfect detection; mammal survey; occupancy; relative abundance index; sampling bias; trail camera; Virginia USA.

Introduction

Since the mid-1990s, camera traps have been employed in an increasingly broad range of ecological studies, addressing questions related to activity patterns, habitat use, and species distribution, with a particular focus on community richness and composition, density, and relative abundance (reviews in O'Connell et al. 2011, Burton et al. 2015). Traditional surveys of terrestrial mammal richness or abundance have relied on designs in which individual transects covered relatively large areas, thereby sampling existing habitat variation at multiple scales (e.g. track counts, scat surveys, distance sampling with sign or observations). While camera traps provide a range of advantages over these traditional methods for sampling select wildlife (Silveira et al. 2003, Tobler et al. 2008), the total area sampled by cameras is notably small, and the information collected therefore has a high potential to be strongly influenced by a range of micro-site characteristics (review in Hofmeester et al. 2019). Questions remain about exactly what area is sampled by a camera trap in a continuous landscape, and how inference should best be made from information collected at a camera site, to the broader landscape (Efford and Dawson 2012, Burton et al. 2015, Neilson et al. 2018).

Camera traps are commonly employed to identify ecological and anthropogenic factors influencing the landscape distribution of species (e.g. Kays et al. 2011, Schuette et al. 2013), (Nagy-Reis et al. 2016, Morin et al. 2018). Given that raw presence/absence information from cameras fails to account for likely spatial and temporal variation in species detection, occupancy models, which utilize repeat site visits estimate detection rates explicitly (MacKenzie et al. 2002), are increasingly used to document habitat use patterns and distribution in camera-based studies (Burton et al. 2015). When applying this framework with camera traps, one must make

two potentially problematic assumptions. First, as in all occupancy frameworks, we assume that detection probability (p) of our sampling device is either constant, or all sources of heterogeneity in p are controlled or explicitly modelled (MacKenzie et al. 2017). For camera traps, an increasingly large list of local site factors have been shown to influence p, many of which impact: 1) the ability to predict or funnel animal movement to the camera (e.g. placement on/off trails: Cusack et al. 2015, Kolowski and Forrester 2017 and roads: Sollmann et al. 2013, Mann et al. 2015; presence of logs: Kolowski and Forrester 2017); 2) the ability to physically detect or see the focal species (e.g. vegetation density: Hofmeester et al. 2017, Kolowski and Forrester 2017, camera detection distance: Hofmeester et al. 2017); or 3) the general favorability of the local site for the species of interest (e.g. local resource availability: Brassine and Parker 2015, presence of bait/lure: Satterfield et al. 2017, Suarez-Tangil and Rodriguez 2017). Although efforts have been made to summarize current knowledge about the factors influencing detection probability of a species (Hofmeester et al. 2019), the ever growing list of potentially important factors should raise doubts as to our ability to identify and measure all the key factors in any given scenario.

Second, camera-based occupancy surveys assume that information collected at the camera location can be associated with broader landscape characteristics. Ecological and anthropogenic variables associated with the camera location, as well as its position in the larger landscape, are used to investigate patterns of site occupancy or use by the focal species (MacKenzie et al. 2017). To maintain independence of site-level information, and often to correlate occupancy with abundance, it has been suggested that the spacing between cameras be based on the size of an animal's home range (e.g. O'Connell and Bailey 2011). While this may be an unnecessary

restriction (MacKenzie et al. 2017) camera-based occupancy sampling designs have tended to adopt this approach, resulting in single cameras being separated by significant distances (0.1 to 5.0 km in Burton et al. 2015). However, little research has been conducted to assess the extent to which data collected at a single point is a consistent and repeatable measure of species occupancy or use at the landscape scale. Those few studies that have compared the effect of sampling single sites with variable numbers of camera stations have found that use of single stations can severely limit detection probability for some species (Stokeld et al. 2016, O'Connor et al. 2017, Evans et al. 2019, Wong et al. 2019) and introduces bias in identification of key ecological factors influencing occupancy (Pease et al. 2016).

Direct information about animal abundance is also critical to wildlife managers and ecologists, and while statistically robust methods are well developed for estimating density of species that can be individually recognized on camera traps (Royle et al. 2015, Borchers and Fewster 2016, Royle et al. 2018), fewer tested options are available for the vast majority of species which do not have distinct individual markings (yet see Rowcliffe et al. 2008, Dénes et al. 2015, Moeller et al. 2018). For species without unique markings there is great interest in using photo capture rate as an index of relative abundance. While robust use of photo rate as an abundance index assumes that photo rate varies consistently and linearly with actual animal abundance (Pollock et al. 2002), those few studies that have investigated this critical assumption have come to varied conclusions (Rovero and Marshall 2009, Sollmann et al. 2013, Parsons et al. 2017, Palmer et al. 2018). Where the index fails, the confounding of abundance and detection is a critical challenge, and robust use of photo rate must necessarily address temporal and spatial variation in detection. A range of models developed to estimate actual abundance from photo count data (e.g. random

encounter model: Rowcliffe et al. 2008, spatial count model: Chandler and Royle 2013, distance sampling model: Howe et al. 2017) are also subject to the same potential confounding effects of factors influencing detection rates, independent of abundance. And while each model has approaches to model variation in detection, a lack of complete knowledge of the factors influencing detection could result in biased estimates.

Our goal was to assess the extent to which capture rate and detection probability data collected at a single camera station are representative of the broader habitat and landscape in which it is placed for a suite of species common to hardwood forests of the northeastern United States. To do so we established a high-density grid of camera traps in homogenous forested habitat, closely controlling camera setup and placement (camera type, height, orientation). Our study investigates the critical, yet often unstated, assumption that photo capture is a reliable indicator of presence and use by a species for a given "site", and therefore capture rates and detection probability should be similar (with necessary allowance for reasonable sampling variation) across multiple cameras at a single site. We therefore assessed variation in capture rate and detection probability at the scale of our grid, which was small enough to be considered a single sampling site (or smaller) for most camera-trap study designs, and compare it to values documented across a much larger surrounding region using a more traditional sampling approach. In addition, we assume there is strong spatial autocorrelation between closely placed cameras within a site and any variation in photo rates should be explainable by measurable local-site characteristics. The study duration allowed us to investigate whether spatial patterns in detection probability and capture/photo rate, and the covariates influencing them, vary across seasons. Our unique design allowed us to ask novel questions about how camera traps sample habitat and species, and what

potential biases may exist when employing this relatively new technology as a wildlife sampling device.

Methods

Study area

We conducted our study on the grounds of the Smithsonian Conservation Biology Institute (SCBI) in Front Royal, Virginia (38.89476, -78.14630). Sixty-six percent of the 1,295-ha property is forested and is contiguous with the nearly 81,000 ha forest of Shenandoah National Park. Forests on the property are varying ages of mixed deciduous forest, with canopies dominated by tulip poplar (*Liriodendron tulipifera*), ash (*Fraxinus spp.*) and a suite of oak (*Quercus spp.*) and hickory (*Carya spp.*) species. Although the SCBI property is fenced, the perimeter fences are permeable to all local wildlife species. The climate is classified as humid subtropical, with hot humid summers and mild cool winters. Snowfall is irregular but common from January through March.

All data collection occurred within a 1-ha section of a larger long-term forest monitoring plot within the ForestGEO network (Bourg et al. 2013, Anderson-Teixeira et al. 2015). Within these monitoring plots, all stems greater than 1 cm diameter at breast height (dbh) are identified to species, tagged, mapped and measured every 5 years. Within our 1 ha focal area, and a 50 m buffer surrounding it, the majority of the more than 3000 woody stems were hickory, tulip poplar, blackgum (*Nyssa sylvatica*), ironwood (*Carpinus caroliniana*), and oak. Our focal site

was roughly bordered on one side by a small, infrequently used gravel road (the broader site is not open to the public), and ranged in elevation from 258-350 m.

Camera grid

We established a dense camera array across this 1 ha area of mature secondary forest, selecting a site with relatively easy access, minimal slope and consistent vegetative structure. The understory was largely open, with high visibility and little dense vegetation. Starting with a random location, we mounted 27 trail cameras at 20 m intervals in offset rows. If there was no tree within 2 m of a placement point, we mounted the camera on a metal post. All cameras faced north and instructions to field staff were to place cameras at knee height, though actual height was varied to account for slope. We set four thin bamboo garden stakes at 2.5, 5, 7.5, and 10 m from the front of the camera to estimate each distance from the camera of detection events (Hofmeester et al. 2017).

We used two Reconyx (Holmern, Wisconsin) camera models, the PC800 HyperFire and the PM75 RapidFire. Both models used Lo-glow, high-output, "semi-covert" infrared night vision, had a 1/10 second trigger speed, and were set to take 5 "rapid-fire" photographs when activated with no quiet period between triggers. We checked the grid every two weeks to replace batteries, reposition cameras if necessary, and replace memory cards nearing capacity. We maintained the grid through four 2-month seasonal deployments: June-July 2017 (summer), October-November 2017 (fall), January-February 2018 (winter), and April-May (spring) 2018.

To compare variation in sampling metrics obtained in our high-resolution grid to variation seen across all study sites in a typical camera trapping study, we took advantage of a previous study conducted in the same area, but spread across a 500 x 500 m resolution sampling grid and covering the full 1300 ha SCBI property (Kolowski and Forrester 2017). As with our small-scale sampling grid, all these sites were restricted to occur in forest, yet they varied in a range of landscape habitat variables (e.g. forest type and age, slope and elevation, distance to edge) and were sampled with two different camera brands. These sites were sampled between June and early December (classified in this study as summer and fall) in 2013 and 2014 and were run for an average of 25 camera-nights. We focus here on two sets of camera samples of 30 (A) and 24 (B) stations that were randomly placed near grid centers to avoid any bias from trails or other features (see Kolowski and Forrester 2017) for more details on field deployments and data processing).

Data processing and summary

Photos from camera deployments were uploaded to the eMammal (www.emammal.si.edu) camera trap management system. Photo sequences were assigned to species by field staff uploading the photos and identifications were then confirmed by experienced staff. Sequence information was then downloaded for analysis, and independent sequences for a given species and camera station were classified as those separated by at least 10 minutes from the previous photo.

We summarized overall presence of each species at the level of the camera and grid for each season and calculated the proportion of the grid's 27 cameras recording each species within a

season. We calculated capture rate at the camera and grid level for each species within and across seasons as: (number of sequences/camera nights) * 100. We calculated summary statistics as well as coefficient of variation (standard deviation/mean) for capture rate for each species and season across the grid. Most analyses focus on the most commonly photographed species to ensure adequate data were available to describe patterns in detection. Because our two diurnal squirrel species, fox squirrel (*Sciurus niger*) and gray squirrel (*Sciurus carolinensis*), are challenging to distinguish in black-and-white nocturnal photos, we typically report results for squirrels both by species, as well as combined with unknown squirrel detections in a third "all squirrels" category.

Small-scale spatial auto-correlation in capture

Most camera-based studies look to ensure that their sampling sites do not display un-modelled spatial correlation in collected data (i.e. the sites offer independent observations), an assumption of most statistical models used with camera data (e.g. occupancy modeling, MacKenzie et al. 2017). In our scenario with small distances separating cameras, we hypothesized that capture rates should be highly correlated, and that this correlation should increase as inter-camera distance decreases. Spatial autocorrelation of capture rates at the level of the entire grid (across all distance combinations) was estimated using Moran's I. To investigate the level of spatial correlation in capture rates at the range of available inter-camera distances, we present correlation values across the range of available distances and examine these patterns visually with correlograms for each species/season combination.

Local site covariates

To examine the possible sources of small-scale variation in capture rate and detection probability within seasons across the grid we attempted to record all locally variable factors that might influence detection rates. A recent review (Hofmeester et al. 2019) summarized the array of factors (independent of abundance) shown or likely to influence camera detection rates. In our controlled scenario we measured the few potential factors that remained. These included: camera height, vegetation density, landscape features channeling animal movement (e.g. trails, logs), and detection area of the camera (Hofmeester et al. 2019). We hypothesized that, although habitat across the grid was fairly homogeneous, minor variation in the density of stems in the viewshed of each camera could influence capture rate and detection. We used the total count of stems within a conical sector loosely representing the viewshed of each camera, and defined by a 40-degree viewing angle extending to 20 m. Here we did not attempt to define the exact viewshed of each camera, but rather to describe the vegetation structure in each camera's broad field of view. We also added a parameter to represent the relative potential quantity of acorns available in each camera's field of view as the sum of the dbh of all oak species in the camera viewshed.

Although our protocol dictated cameras be set at knee height, variation in camera height resulted from a need to adjust for tree shape and angle as well as minor variation in slope. Both large (Meek et al. 2016) and small (Apps and McNutt 2018) changes in camera height have been found to influence detection rates. We therefore measured exact height of each camera as the distance (cm) from the ground to the middle of the camera lens. Recent research has also shown that specific habitat features like logs and trails can have significant impacts on capture rates with camera traps (Kolowski and Forrester 2017), so we also recorded whether each camera

station had a log feature in clear view of the camera. Likely due to the open understory and low slope at our site, there were no obvious game trails in our grid.

Numerous studies have documented the influence of the size of the camera's detection zone on photo capture rate (Rowcliffe et al. 2011, Hofmeester et al. 2017). When estimated, for example to inform density estimation of unmarked species using the Random Encounter Model (Rowcliffe et al. 2008), the detection zone has previously been assumed to be consistent across all camera stations. While variation in local camera setup and surrounding vegetation and structure make this assumption problematic, camera detection distance has never been robustly estimated for individual camera stations. We therefore used a distance sampling (Buckland 2001) approach to estimate effective detection distance (EDD) at each station for as many different species groups as possible. This approach has been used previously to estimate EDD across a camera grid (Hofmeester et al. 2017), but not for individual camera stations. While feasible, it requires that researchers estimate the distance from the camera to each observation, but also that adequate sample sizes can be recorded at each camera to adequately estimate a detection function. In our case, we recorded the distance bin in which the animal was first observed, based on described bamboo markers.

We considered a minimum of 30 observations necessary to adequately describe the detection process at each camera station. We pooled observations at various levels to achieve sufficient sample sizes, first across similar seasons with respect to vegetation (i.e. summer with fall, and winter with spring), then across all 4 seasons when necessary. In some cases pooling was still necessary across groups of similar-sized species to achieve the threshold sample.

Distance sampling analysis was carried out as for point transects with radial distances (Buckland 2001).We used the half-normal key function with potential cosine adjustments to give adequate flexibility in describing the detection functions at each camera. Cut points for analysis bins were listed as 0, 2.5, 5.0, 7.5, 10, and 12.5 m. We ultimately truncated all observations past the furthest marker (10 m). Despite our surveying less than a full circle for each point, no adjustments were made to the size of the area sampled, since density was not being estimated.

Generalized linear modeling of sequence counts

Prior to any modeling, we assessed collinearity among our set of 5 potential predictor variables, considering pairs of covariates with $|r| > 0.7$ highly correlated. In these cases, we kept the covariate of most interest from a research perspective. We next investigated the distributions of our explanatory covariates to check for skew or otherwise problematic patterns and employed any necessary transformations.

Given that our response variable here was the count of independent sequences at each station, we first investigated the potential to model this response in a generalized linear model framework (GLM) with a Poisson error distribution and the associated log link function. Because of the potential for extra-Poisson variation (overdispersion), we estimated overdispersion by running a fully general model (including all non-correlated predictor variables) for each species and season and estimated the overdispersion factor as model deviance divided by the residual degrees of freedom. If overdispersion was detected (overdispersion factor > 1.0), we proceeded with our modeling using a negative binomial distribution to explicitly account for overdispersion (Ver Hoef and Boveng 2007, Zuur 2009). To account for variation in duration of each camera

deployment (e.g. due to occasional malfunction) we ran all models with an offset term (log (deployment duration)).

We then proceeded with a model comparison investigation for each species and season, comparing models based on small sample size corrected AIC values (AICc) and related metrics. Because our sample size was limited by our number of camera stations (n = 27), we limited models (with the exception of initial tests for overdispersion) to a maximum of three covariates. We tested all possible model combinations with this maximum level of complexity (n = 26, including intercept only model). For some species, we modified the set of potential predictor variables to account for specific hypotheses about the observation process. First, we reasoned that for squirrels, which have been shown to be more detectable with logs present in the camera field of view (Kolowski and Forrester 2017), the influence of camera EDD could be altered by the presence of a log, which could be the focal point of detections for these species. Therefore, for each squirrel species (and "all squirrels" group), we first tested a two-variable (log presence and EDD) model with and without an interaction term. If the interaction model was favored based on AICc, all models with both EDD and log presence were run with an interaction term. Finally, we hypothesized that squirrels may be at their most detectable at intermediate camera heights, with cameras too low sacrificing detection distance, and those too high missing nearby individuals altogether. We therefore considered models with a quadratic term on the camera height covariate. If a single covariate model with the quadratic term was favored over the simpler model based on AICc, camera height was thereafter consistently modeled as a quadratic term for that species. Given this, some squirrel models could include up to five parameters (adding either a quadratic term, interaction term, or both).

To assess the amount of variation in capture rates explained by our covariates, we present the explained deviance (model deviance/null model deviance) of the best model (lowest AICc) for each species and season. We also present summed AICc weights across all models including a given covariate (Giam and Olden 2016) to allow an assessment of relative importance of that covariate. For final selected models we conducted standard diagnostic tests including plotting of residuals against predicted values and explanatory variables and investigating points with high leverage using Cook's distance. We discuss any patterns or data points of concern.

To investigate whether season had a significant impact on capture rates, we employed the same modeling approach as above with the same focal species, here comparing a model using season to predict the number of recorded sequences to an intercept-only model using AICc values. In this case each camera could appear in the dataset 4 times for a total potential sample size of 108, and camera was used as a random effect (intercept) to account for the repeated sampling. Season was considered to have an important impact on capture rates if the season model was favored over the intercept only (null) model.

Occupancy modeling to investigate variation in detection probability

In the framework of occupancy modeling, nuisance variation in detection probability (the probability of detecting the species of interest, at an occupied site, on a given sampling occasion) across sites is explicitly estimated and used to reduce bias in estimated site occupancy probabilities (MacKenzie et al. 2017). Model comparison approaches allow identification of the influence of covariates on detection probability. Here detection data are represented in binary

fashion (1 vs. 0) for each sampling occasion, which for camera trap research may range from 1 to multiple days depending on the species and question of interest. Because this simplification of photo sequence data (from total counts to a yes/no per occasion) may reduce the variability among cameras, we first assessed total variation in detection within the grid using summary statistics, as above for capture rate. In this case we calculated raw detection probability for each camera and season as the proportion of occasions (here set to each day) with detections. We then conducted single-species, single-season occupancy models, asking which of our set of covariates influenced detection probability. In this analysis the occupancy parameter was held constant, and we investigated and compared all the same model combinations described above. In this framework each camera station is treated as a site (n = 27).

Effective detection distances for individual cameras were calculated in the program Distance 6.2 (Thomas et al. 2010). All other analyses were conducted in the R computing environment (R Core Team 2019). Correlograms were generated using the package *ncf* (Bjornstad 2019) and Moran's I with package *ape* (Paradis and Schliep 2018). Negative binomial GLM models were run with the package *MASS* (Venables and Ripley 2002) and summarized using the package *AICcmodavg* (Mazerolle 2019). Occupancy models were run in the package *RPresence* (MacKenzie and Hines 2018).

Results

We photographed 15 mammal species within the grid during the full 4-season sampling period across a total of 5569 camera-nights (Figure 1). Two cameras failed entirely in both the fall and winter seasons, resulting in a sample of 25 camera stations for those seasons. The most

commonly photographed species, and those which serve as our focal species for most analyses, were: white-tailed deer (*Odocoileus virginianus,* hereafter "deer"), American black bear (*Ursus americanus,* hereafter, "bear"), eastern gray squirrel (*Sciurus carolinensis*), eastern fox squirrel (*Sciurus niger*) and the northern raccoon (*Procyon lotor,* hereafter "raccoon") as well as unknown small rodents, most of which were likely white-footed mice (*Peromyscus leucopus*). The least captured species across the study were gray fox (*Urocyon cinereoargenteus*), long-tailed weasel (*Mustela frenata*) and southern flying squirrel (*Glaucomys volans*), each of which were captured in only one photo sequence. Total species counts for each season were: 11 in summer, 12 in fall, 13 in winter, and 12 in spring.

Although each of our five focal species were known to occupy our study site throughout the year, only deer were captured at every camera station in every 2-month sampling season (Table 1). Excluding winter and spring for bear, when this species could have been either in torpor or emerging from this state, there were seasons in which multiple cameras failed to register a photo of these common species. This was the case for as many as three cameras for fox squirrel in summer, six for gray squirrel in fall, seven for raccoon in summer, and seven for bear in fall.

Capture rates

Within seasons, we documented high variability in capture rates for all five focal species across the camera grid (Figure 2, Table 1). The highest variability within a season, as represented by the coefficient of variation for capture rate, was for bear in winter, when only two stations detected the species. The next highest variability was for bear in fall (CV = 1.64) where capture rates ranged from 0.00 to 34.99 across the grid. Coefficients of variation were high for all species in

all seasons with a minimum value of 0.45 for deer in spring (Figure 2, Table 1). Variation within our grid across the 4 seasons was broadly similar to that documented across 30 and 24 independent sampling grids on the same property both in terms of the range of values recorded, and the coefficients of variation for most species (Table 1). Few clear patterns emerged in these qualitative comparisons; the variation observed was either higher, lower, or similar in our small sampling grid, depending on the season, species and grid (A vs. B) being compared.

The large range in capture rates for each species within seasons is clear in visual representations of this metric across the grid (Figure 2), with huge differences sometimes evident between neighboring cameras. There was no evidence of global spatial autocorrelation based on Moran's I values (minimum inter-camera distance: 15.8 m; maximum: 114.7 m) for any species in any season except for gray squirrels in summer (Table 2). There was also no evidence of scale-dependent covariance. That is, correlograms indicated consistent values across distance categories from 20m to 80m (e.g. deer, Figure 3), indicating that already at a 20 m separation, capture rate values for these five common species demonstrated independence.

To achieve threshold sample sizes for estimation of EDD, we pooled all squirrel observations and combined data from winter and spring for those seasons (range: 2.2 – 5.2 m), but used pooled 4-season data to estimate EDD for squirrels in summer and fall (range: 2.1 – 5.3 m). For deer, we pooled summer and fall data to estimate values for those seasons (range: 3.0 – 9.0 m). When pooling winter and spring data for deer there remained 5 cameras with less than 30 observations (min 18), but we proceeded with this sample, preferring to maintain seasonal variation in EDD despite the few cameras with low samples (range: 2.9 – 9.4 m). For raccoon, even when pooling across all 4 seasons, 13 cameras failed to meet the 30-observation threshold.

For those cameras with adequate observations we calculated EDD (range: 2.5 – 7.9). For the remaining, we used the EDDs from deer. For all bear analyses we used EDD values for deer.

We considered the number of detections inadequate for regression analysis for bear in winter and spring, and for raccoon in summer. All other species and season combinations were investigated for a total of 21 model-based investigations (including "all squirrels"). Because a single camera site had a particularly high value for stem density, we used a $\log_{10}$ transform for this covariate to improve its distribution for modeling. No other transformations were necessary, and none of the 5 predictor covariates were highly correlated. All fully general models with a Poisson error distribution indicated overdispersion, so we employed a negative binomial error distribution throughout.

The explained deviance (ED) values for the favored models across all species and seasons were generally low (range: 0.0 - 0.50; median = 0.23), with the null (intercept only) model being favored in five of the 21 scenarios, three of which were deer models (Table 3). Models with the highest predictive abilities included that for squirrels in the fall season (ED = 0.50), and fox squirrels in summer (ED = 0.49; Table 3).

Across species, vegetation-based factors featured least frequently in optimal models. The highest summed model weight (SW) for the number of stems in the camera viewshed was 0.61 (scale from 0 to 1) and this was selected in only a single favored model, where increasing stem count reduced the capture rate of fox squirrels in fall. Similarly, the maximum SW for the total dbh of oak trees in the camera viewshed was 0.68, and this parameter was selected in only two best models (reducing raccoon detection in spring and increasing bear detections in fall).

EDD was not an important predictor of capture rate variation in any season for deer or raccoon. Although identified as an important predictor for eight of twelve squirrel scenarios, it was found to reduce detection rates in half of these cases. In the other four, it showed an interaction with log presence where EDD increased capture rate in the absence of logs, but reduced capture rate in the presence of logs (Figure 4).

Camera height, which varied from 33 to 68 cm (median = 53 cm) across the 27 cameras, was not important in predicting capture rates for any of the large-bodied focal species (Table 3). However, increasing camera height did reduce capture rates for all squirrels and fox squirrels in summer (Table 3). This pattern was also detected for raccoons in winter. Only for gray squirrels in winter did we identify a quadratic relationship for camera height (Table 3), where capture rates were highest at an intermediate height of about 53 cm (Appendix S1: Figure S1).

The most consistently important local covariate identified across species models was log presence, which was in 13 of 21 optimal models. For small species (squirrels and raccoon) it had a consistently positive effect on capture rates and figured in the best models for raccoon, gray squirrel and fox squirrel in at least 2 of the 4 seasons (Table 3). Log presence either had no effect, or a negative effect on capture rates for deer and bear.

Capture rates varied to a large degree across the 4 seasons for all our focal species (Table 1, Figure 2) and the season demonstrating the highest mean capture rates was not consistent across species (Table 1). In addition, optimal models explaining capture rate variation were not consistent across seasons for any species (Table 3). For example, whereas EDD, camera height and log presence influenced capture rates for fox squirrels in summer, no covariates explained capture rate variation for this species in winter or spring. There was strong statistical support for

the influence of season on overall capture rates for all species, where models with a season effect were always favored over a null model (Appendix S1: Table S1).

Detection probability/occupancy

Within seasons, as with capture rates, we documented high variability in detection probabilities for all five focal species across the camera grid (Figure 5, Table 4). The highest variability within a season, as represented by the coefficient of variation for capture rate, was for bear in Fall (CV = 1.6), followed by raccoon in summer and gray squirrel in fall. Coefficients of variation were high for all species in all seasons, but lowest values were demonstrated for white-tailed deer in all seasons (range: 0.24-0.37: Figure 5, Table 4). The large range and spatial variation in detection probabilities for each species within seasons is evident across the grid (Figure 5), with huge differences sometimes found between neighboring cameras. When compared to values documented across the larger independent grid sites, as with capture rates, variation was either smaller or larger in our small sampling grid, depending on the season, species and comparison grid (A vs. B) with no strong patterns emerging.

To investigate the influence of local covariates on detection probability (p) we largely replicated the above investigation in an occupancy modeling framework, using single-season, single-species occupancy models. Two changes were made however for the occupancy modeling approach. First, to improve model convergence, we scaled all continuous covariates by subtracting the mean and dividing by the standard deviation. Second, we included the summer season model for raccoons, reasoning there was adequate data available when using the binary detection/non-detection format. Results here were generally consistent with those found for

capture rates with a few notable differences. First, EDD was identified as an important covariate in many more model scenarios (16 of 22), yet it was still inconsistent in its effect (Table 5). For our largest species (deer and bear) the effect, when identified, was often positive (three of four cases). However, as with capture rates, numerous models for squirrels indicated a negative effect of increasing EDD on *p*, and the influence of EDD often depended on whether logs were present (Table 5, Appendix S1: Figure S2).

Whereas vegetation thickness had little influence on overall capture rates, it played a stronger role in determining *p* across a range of species. Notably, increasing vegetation thickness negatively influenced deer detection, where this pattern was not detected for capture rates. Whereas vegetation thickness had no influence on capture rates of raccoon, it had a strong positive influence on *p* for this species all seasons except spring, and this influence was also detected in winter for fox squirrels and all squirrels (Table 5).

Camera height, as for capture rates, had a negative effect on *p* for smaller-sized species in a few model scenarios (Table 5), in some cases with a quadratic relationship (Appendix S1: Figure S1). The important influence of the presence of logs on capture rates was mirrored here for *p*, with a negative influence on larger species and a strong positive influence for smaller species (Table 5).

To compare *p* across seasons for each focal species, we estimated values using the top model in each species:season scenario and mean values for any included covariates, assuming a camera placement without a log in view. As with capture rates, *p* showed significant seasonal variation (Appendix S1: Figure S3) in terms of overall level, as well relative ranking of seasons across species.

Discussion

Ours is the first study to investigate variation in commonly recorded animal sampling metrics with camera traps at a fine spatial resolution, and our design allowed us to ask novel questions about the ability of individual camera traps to sample animal presence and local abundance in a repeatable fashion. We documented large amounts of fine-scale variation in capture rates and detection probabilities for species spanning a large range of trophic levels and body sizes. This variation was demonstrated by high coefficients of variation and large value extremes across our small sampling grid, where in most seasons at least some cameras failed to record a single capture of a common species, whereas nearby cameras displayed frequent captures. Although ostensibly sampling the same habitat with the same devices, we found a near total absence of spatial autocorrelation in capture rates at any distance, for any species in any season, indicating not only was there extreme levels of variation, but that cameras closer together were no more similar than those on opposite ends of the grid.

Some sampling variation is expected with any sampling method, and one would not expect values to be constant. In addition, each individual animal has its own movement patterns, movement rates and habits, and each camera exists at different distances from each animal's center of activity. Indeed, we suspect many of these factors are the underlying cause of some portion of the variation we observed. Yet it is worth noting that the values recorded here for each camera are already the result of averaging 60 separate days of sampling, yet large variation remains. This variation, all documented at a scale most would consider smaller than a single typical sampling site, existed despite strict controls on design not typically implemented in camera sampling designs. Perhaps most surprising was that the level of variation we documented

was comparable to that seen across fully independent forest sampling sites scattered across a 1300 ha study area. These two sets of sites (A and B) used for comparison, while not separated by more common distances of 1-2 km, existed at unique forest locations that varied in a suite of habitat and landscape descriptors. These sites were sampled by two different brands of cameras and were not setup with the strict protocols implemented in our study (height, orientation, etc.). We predicted a much higher variation in sampling metrics to have been displayed in the large-scale sampling design, but no clear pattern in capture rates or detection was observed.

Explaining variation in capture rates and detection probability with covariates

Although the level of variation in capture rates and detection histories we documented was far higher than expected, we anticipated that a significant amount of this variation could be explained by micro-site characteristics measured at each camera station. Although we controlled many factors that may otherwise vary across camera stations in a typical camera-based design (e.g. camera type, camera placement decisions, orientation, and ground cover), and our cameras were all placed in the same habitat type with no more than 115 m separating any two cameras, variation in micro-site vegetation characteristics, camera height, and detection distance still remained. However, these site characteristics generally failed to account for a large percentage of variation in capture rates, as evidenced by low explained deviance of predictive models. In predicting both capture rates and detection probabilities, few factors were identified to be important in predictive models, and even fewer were consistently identified across seasons or species.

The presence of a log feature in the camera view was the most consistently important factor in predicting local variation in capture rate and detection probability with log presence consistently

increasing both metrics for squirrels and raccoons, and in some cases decreasing these metrics for our large species (bears and deer). This pattern has been shown previously in this same habitat and region (Kolowski and Forrester 2017), but we are aware of no other studies that have investigated the importance of logs or other structural features on detection metrics. The importance of this feature was more consistent in summer and fall, the seasons when vegetation cover is highest. This may indicate that smaller species utilize these features to facilitate movement, as appeared to be the case in previous work (Kolowski and Forrester 2017), yet understory vegetation was generally sparse in our study grid. It is therefore more likely that these features facilitate detection by the cameras by bringing smaller species like squirrels into clearer view and improving identification by those reviewing photos. Regardless, any studies interpreting capture rate or detection probability data should note the presence of structural features in the camera view, as they can strongly influence photo sequence counts, particularly for smaller species.

We anticipated that camera effective detection distance (EDD) would play an important role in explaining small-scale variation in capture rates and detection probability. Logically, cameras with a larger EDD, resulting from minor variation in slope, camera angle and habitat structure, should capture more animal events and at least on a landscape scale, cameras with more obstructed viewsheds have been found to capture fewer detections of nearly all our focal species (Moll et al. 2020). Ours is the first study to our knowledge to successfully measure EDD of individual camera stations, and this provided a unique opportunity to assess its influence, in a controlled scenario. To our surprise EDD failed to explain any significant variation in capture rate for either deer or raccoon, and although identified to influence deer detection probabilities, its effect was reversed between summer and winter. EDD did influence squirrel capture rates and

detection probabilities, yet its influence here was more complicated, varying by season and with log presence. It is likely that when logs are present the log and foreground become a focal point for detections. In the absence of log features, cameras that can see farther capture more events. Only for bears was the influence of EDD consistently positive for both capture rates and detection probabilities.

The importance of EDD across a range of species (despite its varied direction of effect), and the range of values we recorded despite the controlled design, implies that this variable should be estimated for studies investigating patterns in captures rates or attempting to account for variation in detection probability (i.e. occupancy models). At least one project has recorded maximum detection distance at each camera station, walking themselves at decreasing distances from the camera (Kays et al. 2016). While simpler to record, it is unclear how well this metric corresponds to actual EDD, and it fails to account for interspecific variation in detection distance. We found that cameras with high EDD for deer were not necessarily those with high EDD for squirrel species (winter/spring Pearson $r = 0.21$). While methods are well described to measure the full detection zone of camera traps (Rowcliffe et al. 2008, Rowcliffe et al. 2011, Caravaggi et al. 2016) these require measurements additional to those collected here, and the method by Hofmeester et al. (2017) utilized here has been shown to correlate well with these more rigorous measures. Unfortunately, estimation for each camera requires substantial captures of each species at each camera station, and we were forced here in some cases to pool observations across different seasons which may themselves influence EDD. In working toward a practical and validated metric of EDD, research should attempt to confirm whether a human-based maximum detection distance method, or those that estimate obstruction of the camera viewshed (e.g. Moll et al. 2020) would correlate well with more rigorous distance-sampling data

as analyzed here. Given the recent development of distance sampling approaches to estimated density of unmarked animals (Howe et al. 2017), there may be additional justification to set distance marking poles at camera stations, depending on research objectives.

It seems reasonable to assume that as vegetation density increases, detections would decrease. Although few studies have incorporated this parameter into modeling of capture rates or detection probabilities, perhaps due to the additional time necessary to record it, there is evidence that increasing either the understory vegetation density (Kolowski and Forrester 2017) or obstruction of the camera viewshed (Moll et al. 2020) reduces detections for a range of mammal species in eastern North America. In addition, Hofmeester et al. (2017) found that EDD declined for numerous species in dense compared to open understory in forests of the Netherlands. Yet in our study overall, the role of vegetation density was equivocal, with negligible impact on capture rates, and variable impact on detection probabilities, in some cases strongly improving detection and in other cases strongly reducing it. It is notable that vegetation density does have the ability to influence not only the detection abilities of the camera, but also the local site favorability for use by different species, making it particularly challenging to categorize its broad effects on animal capture. This factor may prove more important where trails are used for camera placement as trail use may correlate with vegetation thickness (Kolowski and Forrester 2017). In addition, understory in our study grid was sparse overall and this may have broadly limited the impact of vegetation density.

Spatial autocorrelation

Any research project using cameras to sample animal populations and basing inference on sequence counts or occasion-based detection probabilities should aim to have each site exist as

an independent sampling unit. That is, the data collected at one site should not be influenced by or related to that collected at any other site, with the most concern coming from cameras near each other. Our results indicate that cameras would have to be extremely close to violate assumptions of independence for capture rates. Although few studies have investigated spatial autocorrelation at small scales, those that have were similarly unable to document spatial autocorrelation in capture rates down to distances of 200m (Blake and Loiselle 2018), and as low as 25m (Kays et al. 2011). For the vast majority of the 20 study sites surveyed by Parsons et al. (2017), male white-tailed deer capture rates were estimated to be independent at distances well below their minimum camera spacing of 50m. Even at 20m, we were unable to detect similarities in capture rate for any of our focal species in any season with only one exception (gray squirrel in fall). While this is encouraging from the standpoint of meeting basic assumptions of most statistical analyses, it should also be a significant concern that even cameras very close to each other are not displaying similar sampling metrics.

Seasonal variation

Mean capture rates and detection probabilities varied widely across seasons for all 5 focal species. This was expected for black bear, who seasonally enter a state of severely reduced activity (torpor) in winter, but not necessarily for the other focal species. Overall this topic has received relatively little attention in the literature. Kays et al. (2020) found capture rates to vary as much as 4-5 times for seasonally sensitive species in temperate climates, and this effect was evident at a global scale as well, with 37-50% of species demonstrating significant variation in occupancy or detection rates across seasons. Cusack et al. (2015) also found capture rates for individual species to vary between wet and dry seasons. Given that patterns of detection were largely inconsistent across seasons, care should be taken in pooling data across seasons and

studies planning to compare detection metrics across areas or times should make all attempts to control for season variation. Unfortunately, the impact of season on species capture rates may not be consistent, even within the same broad ecosystems. Whereas no seasonal differences in capture rates were detected in North Carolina for deer, squirrel or raccoon (Kays et al. 2020), we found significant seasonal differences for all three species, though the differing scales of the two studies may be relevant.

Design Recommendations

Particularly in the context of occupancy investigations, the definition of a site is a key decision for study design. Given that camera traps are typically used to survey continuous habitat, the definition of a site can be challenging (Efford and Dawson 2012) and two approaches are available: the sampling site can be defined strictly as the area within the detection zone of the camera (i.e. a point sample), or as some larger plot (e.g. defined by a regular grid) in which single or multiple cameras are placed (Efford and Dawson 2012, Wearn and Glover-Kapfer 2017). Whereas plot/grid-based designs allow additional flexibility in camera placement and could include multiple cameras or sampling methods, a point-based definition is often favored for camera studies due to the lack of reliance on potentially arbitrary plot sizes, which influence occupancy estimates and limit comparison across studies (Wearn and Glover-Kapfer 2017). The point-based design also allows appropriate interpretation of occupancy as proportion of area occupied by the species, which is problematic with a grid/plot-based design (Efford and Dawson 2012).

While a site definition based on the camera's detection zone has various advantages, our study shows that the data collected may not be a representative or repeatable survey of species

presence or local use of the location in which this point sits. Point-based designs may benefit from a recently described approach using the time-lapse setting available on most camera traps as a novel way to minimize bias associated with interspecies or inter-site detection probability variation (Moeller et al. 2018). This approach should severely limit the influence of species characteristics (e.g. size, movement speed), detection distance, and potentially camera height on detection probabilities. Importantly though, this approach will not reduce the role of micro-site parameters that influence the likelihood that a species will use the area in the viewshed of the camera, and we show here that potentially unknown parameters in this category may be causing large site to site variation in capture rates across very small distances.

Our data suggest that any grid/plot-based projects should consider a multi-camera approach within each grid cell or sampling site to minimize the influence of unmeasured, or unknown micro-site factors. It is assumed that observations obtained from a surveyed area, in this case the detection zone of a camera, are representative of the sampled site (MacKenzie et al. 2017), and our data indicate information from a single camera is unlikely to meet this assumption when a site is defined as an area larger than the camera's field of view. In addition, a multi-camera approach has been shown, particularly for elusive species, to be a cost-efficient approach (Galvez et al 2016), and to result in significant improvements in detection probability (Stokeld et al. 2016, O'Connor et al. 2017, Evans et al. 2019, Wong et al. 2019), which should reduce bias in occupancy estimates (MacKenzie and Royle 2005, Bailey et al. 2007, Guillera-Arroita et al. 2010, Neilson et al. 2018) and potentially offset any reductions in total number of sites samples (MacKenzie et al. 2017). Recent work with multi-camera sampling supports this, where conclusions about occupancy with single cameras were different from those based on the full multi-camera design (Pease et al. 2016) and multi-camera sampling increases precision of

occupancy estimates (Wong et al. 2019). An attractive yet underutilized analytical approach for handling presence/absence data collected using multiple cameras at each sample site is the multi-method/multi-scale occupancy model (Nichols et al. 2008), which is parameterized to account for the lack of independence in data from multiple sampling methods at sites. Separate cameras within sites could be set randomly, or could target distinct micro-habitats (e.g. dense vs. open understory) or placement approaches (e.g. log, trail, random) and estimation of unique detection probabilities for these placements would be possible (Nichols et al. 2008).

With respect to interpretation of sequence counts/capture rates, either among species or between study areas, our data adds to the concerns already existing in the literature (e.g. Jennelle et al. 2002, Sollmann et al. 2013, Anile and Devillard 2016) about the extent to which these values should be used for inference about relative abundance. It seems clear from our results that any interpretation or modeling of sequence counts or capture rates must include covariates representing the local site conditions, including structural complexity in the camera view and at least some index for detection distance. As above, the addition of multiple cameras to represent an average capture rate or sequence count for each sampling site may be helpful to minimize bias associated with individual locations. This approach should also be considered for more recent methods looking to estimate abundance for unmarked animals based on count data from cameras (e.g. N-mixture models: Royle 2004, spatial count model: Chandler and Royle 2013).

Conclusions

A robust sampling approach for animal site occurrence or relative abundance should be repeatable and consistent, in that data collected using the same methodology, in nearby locations, and/or very similar habitat should yield similar results. This assumption is rarely questioned for camera trap studies. Our study indicates single camera stations may fail to sample animal

presence and frequency of use in a robust and repeatable way, primarily resulting from the influence of micro-site characteristics and the movements patterns of individual animals. Researchers employing camera traps, particularly when interpretation of capture rate or detection probability is critical to proper inference, must recognize the extent to which collected data may be influenced by local characteristics and animal idiosyncrasies, and should employ multiple cameras at a sample site, more comprehensive sets of model covariates, or other strategic design and modeling approaches.

Acknowledgements

We thank the following interns in the Conservation Ecology Center at the Smithsonian Conservation Biology Institute for their assistance in setting and maintaining the camera traps, and uploading camera data: Katherine Rola, Dwight Wilson, Sarah Macey, Jacob Kraus, Lauren Bowman, Abigal Ferson, Caroline Kittle, Ian McGregor, Michael Scott, Jonathan Stutzman. We thank Jen Zhao for her assistance with data management through the eMammal system, and Valentine Herrmann for assistance with R coding. Finally, we thank Grant Connette and the anonymous reviewers who have contributed to the improvement of this article.

Literature Cited

Anderson-Teixeira, K. J., S. J. Davies, A. C. Bennett, E. B. Gonzalez-Akre, H. C. Muller-Landau, S. Joseph Wright, K. Abu Salim, A. l. M. Almeyda Zambrano, A. Alonso, J. L. Baltzer, Y. Basset, N. A. Bourg, E. N. Broadbent, W. Y. Brockelman, S. Bunyavejchewin, D. F. R. P. Burslem, N. Butt, M. Cao, D. Cardenas, G. B. Chuyong, K. Clay, S. Cordell, H. S. Dattaraja, X. Deng, M. Detto, X. Du, A. Duque, D. L. Erikson, C. E. N. Ewango, G. A. Fischer, C. Fletcher, R. B. Foster, C. P. Giardina, G. S. Gilbert, N. Gunatilleke, S. Gunatilleke, Z. Hao, W. W. Hargrove, T. B. Hart, B. C. H. Hau, F. He, F. M. Hoffman, R. W. Howe, S. P. Hubbell, F. M. Inman-Narahari, P. A. Jansen, M. Jiang, D. J. Johnson, M. Kanzaki, A. R. Kassim, D. Kenfack, S. Kibet, M. F. Kinnaird, L. Korte, K. Kral, J. Kumar, A. J. Larson, Y. Li, X. Li, S. Liu, S. K. Y. Lum, J. A. Lutz, K. Ma, D. M. Maddalena, J.-R. Makana, Y. Malhi, T. Marthews, R. Mat Serudin, S. M. McMahon, W. J. McShea, H. R. Memiaghe, X. Mi, T. Mizuno, M. Morecroft, J. A. Myers, V. Novotny, A. A. de Oliveira, P. S. Ong, D. A. Orwig, R. Ostertag, J. den Ouden, G. G. Parker, R. P. Phillips, L. Sack, M. N. Sainge, W. Sang, K. Sri-ngernyuang, R. Sukumar, I.-F. Sun, W. Sungpalee, H. S. Suresh, S. Tan, S. C. Thomas, D. W. Thomas, J. Thompson, B. L. Turner, M. Uriarte, R. Valencia, M. I. Vallejo, A. Vicentini, T. Å. VrÅ¡ka, X. Wang, X. Wang, G. Weiblen, A. Wolf, H. Xu, S. Yap, and J. Zimmerman. 2015. CTFS-ForestGEO: a worldwide network monitoring forests in an era of global change. Global Change Biology 21:528-549.

Anile, S., and S. Devillard. 2016. Study design and body mass influence RAIs from camera trap studies: evidence from the Felidae. Animal Conservation 19:35-45.

Apps, P., and J. W. McNutt. 2018. Are camera traps fit for purpose? A rigorous, reproducible and realistic test of camera trap performance. African Journal of Ecology 56:710-720.

Bailey, L. L., J. E. Hines, J. D. Nichols, and D. I. MacKenzie. 2007. Sampling design trade-offs in occupancy studies with imperfect detection: examples and software. Ecological Applications 17:281-290.

Bjornstad, O. N. 2019. ncf: Spatial covariance functions. R package. Version 1.2-8. https://CRAN.R-project.org/package=ncf. *in*.

Blake, J. G., and B. A. Loiselle. 2018. Annual and spatial variation in composition and activity of terrestrial mammals on two replicate plots in lowland forest of eastern Ecuador. PeerJ 6:e4241.

Borchers, D., and R. Fewster. 2016. Spatial capture-recapture models. Statistical Science 31:219-232.

Bourg, N. A., W. J. McShea, J. R. Thompson, J. C. McGarvey, and X. Shen. 2013. Initial census, woody seedling, seed rain, and stand structure data for the SCBI SIGEO Large Forest Dynamics Plot. Ecology 94:2111-2111.

Brassine, E., and D. Parker. 2015. Trapping elusive cats: Using intensive camera trapping to estimate the density of a rare African felid. Plos One 10:e0142508.

Buckland, S. T. 2001. Introduction to distance sampling: estimating abundance of biological populations. Oxford University Press, Oxford, UK.

Burton, A. C., E. Neilson, D. Moreira, A. Ladle, R. Steenweg, J. T. Fisher, E. Bayne, and S. Boutin. 2015. Wildlife camera trapping: a review and recommendations for linking surveys to ecological processes. Journal of Applied Ecology 52:675-685.

Caravaggi, A., M. Zaccaroni, F. Riga, S. C. Schai-Braun, J. T. A. Dick, W. I. Montgomery, and N. Reid. 2016. An invasive-native mammalian species replacement process captured by

camera trap survey random encounter models. Remote Sensing in Ecology and Conservation 2:45-58.
Chandler, R. B., and J. A. Royle. 2013. Spatially explicit models for inference about density in unmarked or partially marked populations. The Annals of Applied Statistics 7:936-954.
Cusack, J. J., A. J. Dickman, J. M. Rowcliffe, C. Carbone, D. W. Macdonald, and T. Coulson. 2015. Random versus game trail-based camera trap placement strategy for monitoring terrestrial mammal communities. Plos One 10:e0126373.
Dénes, F. V., L. F. Silveira, S. R. Beissinger, and N. Isaac. 2015. Estimating abundance of unmarked animal populations: accounting for imperfect detection and other sources of zero inflation. Methods in Ecology and Evolution 6:543-556.
Efford, M. G., and D. K. Dawson. 2012. Occupancy in continuous habitat. Ecosphere 3:32.
Evans, B. E., C. E. Mosby, and A. Mortelliti. 2019. Assessing arrays of multiple trail cameras to detect North American mammals. Plos One 14:e0217543.
Giam, X., and J. D. Olden. 2016. Quantifying variable importance in a multimodel inference framework. Methods in Ecology and Evolution 7:388-397.
Guillera-Arroita, G., M. S. Ridout, and B. J. T. Morgan. 2010. Design of occupancy studies with imperfect detection. Methods in Ecology and Evolution 1:131-139.
Hofmeester, T. R., J. P. G. M. Cromsigt, J. Odden, H. Andrén, J. Kindberg, and J. D. C. Linnell. 2019. Framing pictures: A conceptual framework to identify and correct for biases in detection probability of camera traps enabling multi-species comparison. Ecology and Evolution 9:2320-2336.
Hofmeester, T. R., J. M. Rowcliffe, and P. A. Jansen. 2017. A simple method for estimating the effective detection distance of camera traps. Remote Sensing in Ecology and Conservation 3:81-89.
Howe, E. J., S. T. Buckland, M.-L. Després-Einspenner, H. S. Kühl, and J. Matthiopoulos. 2017. Distance sampling with camera traps. Methods in Ecology and Evolution 8:1558-1565.
Jennelle, C. S., M. C. Runge, and D. I. MacKenzie. 2002. The use of photographic rates to estimate densities of tigers and other cryptic mammals: a comment on misleading conclusions. Animal Conservation 5:119-120.
Kays, R., B. Arborgast, M. C. Baker-Whatton, C. Beirne, H. Boone, M. Bowler, S. Burneo, M. V. Cove, P. Ding, S. Espinosa, A. Gonçalves, C. Hansen, P. A. Jansen, J. M. Kolowski, T. Knowles, M. Lima, J. J. Millspaugh, W. J. McShea, K. Pacifici, A. W. Parsons, B. S. Pease, F. Rovero, F. Santos, S. Schuttler, D. Sheil, X. Si, M. Snider, and W. Spironello. 2020. An empirical evaluation of camera trap study design: how many, how long, and when? Methods in Ecology and Evolution 11:700-713.
Kays, R., A. W. Parsons, M. C. Baker, E. L. Kalies, T. Forrester, R. Costello, C. T. Rota, J. J. Millspaugh, W. J. McShea, and J. Toit. 2016. Does hunting or hiking affect wildlife communities in protected areas? Journal of Applied Ecology 54:242-252.
Kays, R., S. Tilak, B. Kranstauber, P. A. Jansen, and C. Carbone. 2011. Monitoring wild animal communities with arrays of motion sensitive camera traps. International Journal of Research and Reviews in Wireless Sensor Networks 1:19-29.
Kolowski, J. M., and T. D. Forrester. 2017. Camera trap placement and the potential for bias due to trails and other features. Plos One 12:e0186679.
MacKenzie, D. I., and J. E. Hines. 2018. RPresence: R interface for program PRESENCE. R package version 2.12.31.

MacKenzie, D. I., J. D. Nichols, G. B. Lachman, S. Droege, J. A. Royle, and C. A. Langtimm. 2002. Estimating site occupancy rates when detection probabilities are less than one. Ecology 83:2248-2255.

MacKenzie, D. I., J. D. Nichols, J. A. Royle, K. H. Pollock, L. L. Bailey, and J. E. Hines. 2017. Occupancy Estimation and Modeling. Second edition. Academic Press, Boston, Massachusetts, USA.

MacKenzie, D. I., and J. A. Royle. 2005. Designing occupancy studies: General advice and allocating survey effort. Journal of Applied Ecology 42:1105-1114.

Mann, G. K. H., M. J. O'Riain, and D. M. Parker. 2015. The road less travelled: assessing variation in mammal detection probabilities with camera traps in a semi-arid biodiversity hotspot. Biodiversity and Conservation 24:531-545.

Mazerolle, M. J. 2019. AICcmodavg: Model selection and multimodel inference based on (Q)AIC(c). R package version 2.2-2. https://cran.r-project.org/package=AICcmodavg.

Meek, P. D., G. A. Ballard, and G. Falzon. 2016. The higher you go the less you will know: placing camera traps high to avoid theft will affect detection. Remote Sensing in Ecology and Conservation 2:204-211.

Moeller, A. K., P. M. Lukacs, and J. S. Horne. 2018. Three novel methods to estimate abundance of unmarked animals using remote cameras. Ecosphere 9:e02331.

Morin, D. J., D. B. Lesmeister, C. K. Nielsen, and E. M. Schauber. 2018. The truth about cats and dogs: Landscape composition and human occupation mediate the distribution and potential impact of non-native carnivores. Global Ecology and Conservation 15:e00413.

Nagy-Reis, M. B., J. D. Nichols, A. G. Chiarello, M. C. Ribeiro, and E. Z. F. Betz. 2016. Landscape Use and Co-Occurrence Patterns of Neotropical Spotted Cats. Plos One 12:e0168441.

Neilson, E. W., T. Avgar, A. C. Burton, K. Broadley, and S. Boutin. 2018. Animal movement affects interpretation of occupancy models from camera-trap surveys of unmarked animals. Ecosphere 9:e02092.

Nichols, J. D., L. L. Bailey, A. F. O'Connell, N. W. Talancy, E. H. C. Grant, A. T. Gilbert, E. M. Annand, T. P. Husband, and J. E. Hines. 2008. Multi-scale occupancy estimation and modelling using multiple detection methods. Journal of Applied Ecology 45:1321-1329.

O'Connell, A., and L. L. Bailey. 2011. Inference for occupancy and occupancy dynamics. Pages 191-204 *in* A. F. O'Connell, J. D. Nichols, andK. U. Karanth, editors. Camera traps in animal ecology: methods and analyses. Springer,Tokyo.

O'Connell, A., J. D. Nichols, and K. U. Karanth, editors. 2011. Camera traps in animal ecology: methods and analyses. Springer, Tokyo.

O'Connor, K. M., L. R. Nathan, M. R. Liberati, M. W. Tingley, J. C. Vokoun, and T. A. G. Rittenhouse. 2017. Camera trap arrays improve detection probability of wildlife: Investigating study design considerations using an empirical dataset. Plos One 12:e0175684.

Palmer, M. S., A. Swanson, M. Kosmala, T. Arnold, and C. Packer. 2018. Evaluating relative abundance indices for terrestrial herbivores from large-scale camera trap surveys. African Journal of Ecology 56:791-803.

Paradis, E., and K. Schliep. 2018. ape 5.0: an environment for modern phylogenetics and evolutionary analyses in R. Bioinformatics 35:526-528.

Parsons, A. W., T. Forrester, W. J. McShea, M. C. Baker-Whatton, J. J. Millspaugh, and R. Kays. 2017. Do occupancy or detection rates from camera traps reflect deer density? Journal of Mammalogy 98:1547-1557.

Pease, B. S., C. K. Nielsen, and E. J. Holzmueller. 2016. Single-camera trap survey designs miss detections: Impacts on estimates of occupancy and community metrics. Plos One 11:e0166689.

Pollock, K. H., J. D. Nichols, T. R. Simons, G. L. Farnsworth, L. L. Bailey, and J. R. Sauer. 2002. Large scale wildlife monitoring studies: statistical methods for design and analysis. Environmetrics 13:105-119.

R Core Team. 2019. R: A language and environment for statistical computing. *in* R Foundation for Statistical Computing,Vienna, Austria.

Rovero, F., and A. R. Marshall. 2009. Camera trapping photographic rate as an index of density in forest ungulates. Journal of Applied Ecology 46:1011-1017.

Rowcliffe, J. M., C. Carbone, P. A. Jansen, R. Kays, and B. Kranstauber. 2011. Quantifying the sensitivity of camera traps: an adapted distance sampling approach. Methods in Ecology and Evolution 2:464-476.

Rowcliffe, J. M., J. Field, S. T. Turvey, and C. Carbone. 2008. Estimating animal density using camera traps without the need for individual recognition. Journal of Applied Ecology 45:1228-1236.

Royle, J. A. 2004. N-mixture models for estimating population size from spatially replicated counts. Biometrics 60:108-115.

Royle, J. A., A. K. Fuller, and C. Sutherland. 2018. Unifying population and landscape ecology with spatial capture-recapture. Ecography 41:444-456.

Royle, J. A., C. Sutherland, A. K. Fuller, and C. C. Sun. 2015. Likelihood analysis of spatial capture-recapture models for stratified or class structured populations. Ecosphere 6:22.

Satterfield, L. C., J. J. Thompson, A. Snyman, L. Candelario, B. Rode, and J. P. Carroll. 2017. Estimating occurrence and detectability of a carnivore community in eastern Botswana using baited camera traps. African Journal of Wildlife Research 47:32-46.

Schuette, P., A. P. Wagner, M. E. Wagner, and S. Creel. 2013. Occupancy patterns and niche partitioning within a diverse carnivore community exposed to anthropogenic pressures. Biological Conservation 158:301-312.

Silveira, L., A. T. A. Jacomo, and J. A. F. Diniz. 2003. Camera trap, line transect census and track surveys: a comparative evaluation. Biological Conservation 114:351-355.

Sollmann, R., A. Mohamed, H. Samejima, and A. Wilting. 2013. Risky business or simple solution - Relative abundance indices from camera-trapping. Biological Conservation 159:405-412.

Stokeld, D., A. S. K. Frank, B. Hill, J. L. Choy, T. Mahney, A. Stevens, S. Young, D. Rangers, W. Rangers, and G. R. Gillespie. 2016. Multiple cameras required to reliably detect feral cats in northern Australian tropical savanna: an evaluation of sampling design when using camera traps. Wildlife Research 42:642-649.

Suarez-Tangil, B. D., and A. Rodriguez. 2017. Detection of Iberian terrestrial mammals employing olfactory, visual and auditory attractants. European Journal of Wildlife Research 63:93.

Thomas, L., S. T. Buckland, E. A. Rexstad, J. L. Laake, S. Strindberg, S. L. Hedley, R. B. B. Jon, T. A. Marques, and K. P. Burnham. 2010. Distance software: Design and analysis of

distance sampling surveys for estimating population size. Journal of Applied Ecology 47:5-14.
Tobler, M. W., S. E. Carrillo-Percastegui, R. L. Pitman, R. Mares, and G. Powell. 2008. An evaluation of camera traps for inventorying large- and medium-sized terrestrial rainforest mammals. Animal Conservation 11:169-178.
Venables, W. N., and B. D. Ripley. 2002. Modern applied statistics with S. Springer, New York.
Ver Hoef, J. M., and P. L. Boveng. 2007. Quasi-Poisson vs. negative binomial regression: How should we model overdispersed count data? Ecology 88:2766-2772.
Wearn, O. R., and P. Glover-Kapfer. 2017. Camera-trapping for conservation: a guide to best practices. *in* WWF Conservation Technology Series. WWF-UK,Wokong, United Kingdom.
Wong, S. T., J. L. Belant, R. Sollmann, A. Mohamed, J. Niedballa, J. Mathai, G. M. Street, and A. Wilting. 2019. Influence of body mass, sociality, and movement behavior on improved detection probabilities when using a second camera trap. Global Ecology and Conservation 20:e00791.
Zuur, A. F. 2009. Mixed effects models and extensions in ecology with R. Springer, London/New York

Tables

Table 1. Mean, standard deviation (SD), minimum and maximum capture rates (# of photo sequences/# days of deployment *100), coefficient of variation (CV = SD/mean) in capture rate, and proportion of cameras with detections, recorded for five focal species for each of four seasons in a high-density camera grid with 27 camera stations. A "total" category shows data when seasons are pooled, with each camera described by an overall capture rate. For comparison, values obtained from a previous study (SCBI Forest Grid), based on 30 (A) and 24 (B) camera stations at 500m grid separation are also shown.

Species and Season	Mean	SD	Min	Max	CV	Prop. of cameras detecting species
White-tailed deer (total)	89.03	88.03	3.33	461.82	1.01	1.0 (104/104)
Summer	61.88	30.50	21.31	159.43	0.49	1.0 (27/27)
Fall	204.78	108.88	34.98	461.82	0.53	1.0 (25/25)
Winter	58.55	36.35	12.27	164.83	0.62	1.0 (25/25)
Spring	37.24	16.68	3.33	79.71	0.45	1.0 (27/27)
SCBI Forest Grid A	*53.51*	*53.66*	*4.17*	*216.67*	*1.00*	
SCBI Forest Grid B	*35.64*	*25.70*	*0.00*	*90.48*	*0.72*	
Fox squirrel (total)	31.65	28.77	0.00	135.20	1.10	0.95 (99/104)
Summer	10.52	11.11	0.00	37.70	1.06	0.88 (24/27)
Fall	20.06	17.62	0.00	81.61	0.88	0.92 (23/25)
Winter	41.59	29.46	5.26	112.10	0.71	1.0 (25/25)
Spring	54.29	29.11	12.13	135.20	0.54	1.0 (27/27)
SCBI Forest Grid A	*1.12*	*3.61*	*0.00*	*151.79*	*3.21*	
SCBI Forest Grid B	*0.36*	*1.77*	*0.00*	*8.70*	*4.90*	
Gray squirrel (total)	21.04	24.90	0.00	105.70	0.85	0.88 (91/104)
Summer	5.77	6.12	0.00	22.95	1.06	0.85 (23/27)
Fall	11.31	16.36	0.00	63.51	1.45	0.76 (19/25)
Winter	18.17	19.90	0.00	63.11	1.10	0.88 (22/25)
Spring	47.98	26.66	10.40	105.70	0.56	1.0 (27/27)
SCBI Forest Grid A	*14.00*	*25.50*	*0.00*	*86.05*	*1.82*	
SCBI Forest Grid B	*16.10*	*35.50*	*0.00*	*163.64*	*2.20*	
Northern raccoon (total)	16.29	20.87	0.00	138.55	0.78	0.91 (95/104)
Summer	3.45	4.5	0.00	19.67	1.31	0.74 (20/27)
Fall	16.23	13.23	0.00	46.80	0.81	0.92 (23/25)
Winter	34.82	32.25	3.51	138.55	0.93	1.0 (25/25)
Spring	12.04	7.97	3.47	29.46	0.66	1.0 (27/27)
SCBI Forest Grid A	*24.63*	*30.04*	*0.00*	*109.30*	*1.22*	
SCBI Forest Grid B	*22.28*	*23.22*	*0.00*	*100.00*	*1.04*	
Black bear (total)	3.40	5.10	0.00	34.99	0.67	0.60 (62/104)
Summer	6.76	4.39	0.00	16.39	0.65	0.96 (26/27)
Fall	4.61	7.53	0.00	34.99	1.64	0.72 (18/25)
Winter	0.19	0.69	0.00	3.03	3.60	0.08 (2/25)
Spring	1.91	2.41	0.00	10.79	1.26	0.59 (16/27)

SCBI Forest Grid A	*6.95*	*9.89*	*0.00*	*42.86*	*1.42*
SCBI Forest Grid B	*7.72*	*9.10*	*0.00*	*36.36*	*1.18*

Table 2. Observed Moran's I values across the camera grid along with *p* values for each species in each season. Expected values are shown in column headings for each season and significant values are shown in bold.

Species	Summer (Exp = -0.0385)		Fall (Exp = -0.0417)		Winter (Exp = -0.0417)		Spring (Exp = -0.0385)	
	Obs	*p*	Obs	*p*	Obs	*p*	Obs	*p*
White-tailed deer	-0.027	0.66	-0.018	0.41	-0.004	0.18	-0.006	0.24
Fox squirrel	-0.062	0.38	-0.072	0.24	-0.018	0.41	-0.046	0.77
Gray squirrel	**0.024**	**0.02**	-0.053	0.67	-0.020	0.45	0.003	0.14
All squirrels	-0.048	0.73	-0.070	0.31	-0.062	0.48	-0.062	0.39
Northern raccoon	-0.032	0.79	-0.042	0.99	-0.047	0.84	-0.034	0.86
Black bear	0.014	0.38	-0.030	0.61	-	-	0.002	0.09

Table 3. Cumulative Model Weights for five covariates tested against number of camera sequences with offset of effort for 27 stations in each of four seasons for five focal species. Covariates include effective detection distance (EDD), camera height in cm (Height), dbh of oak trees in camera viewshed (Oak), total number of stems in camera viewshed (Stems) and the presence/absence of a log in the camera viewshed (Log). Also shown are explained deviances (ED) for both the favored model (lowest AICc) and the full model for comparison. Those covariates selected in the top model are shown in bold and the sign of the coefficient(s) in the top models are indicated after each summed model weight. When no covariates are in bold, the intercept only model was that with the lowest AICc value.

Species-Season	ED_best	ED_full	EDD	Height	Oak	Stems	Log
Deer - Summer	0.38	0.45	0.23	0.18	0.19	0.35	**0.97 (-)**
Deer - Fall	0.00	0.12	0.19	0.38	0.24	0.21	0.27
Deer - Winter	0.00	0.10	0.19	0.20	0.21	0.44	0.22
Deer - Spring	0.00	0.13	0.19	0.22	0.40	0.25	0.30
All Squirrel - Summer	0.48	0.50	**0.74 (-)**	**0.63 (-)**	0.11	0.11	**0.91 (+)**
All Squirrel - Fall†	0.50	0.50	**0.71 (x)**	0.18	0.17	0.17	**0.82 (+)**
All Squirrel - Winter†	0.14	0.29	0.22	0.18	0.20	0.24	**0.62 (+)**
All Squirrel - Spring†	0.33	0.38	**0.53 (x)**	0.16	0.19	0.29	**0.72 (+)**
Fox Squirrel – Summer	0.49	0.54	**0.88 (-)**	**0.40 (-)**	0.10	0.20	**0.87 (+)**
Fox Squirrel – Fall	0.44	0.46	**0.77 (-)**	0.15	0.12	**0.61 (-)**	**0.74 (+)**
Fox Squirrel – Winter	0.00	0.06	0.19	0.19	0.10	0.20	0.27
Fox Squirrel - Spring#	0.00	0.26	0.24	0.39	0.29	0.18	0.22
Gray Squirrel – Summer	0.30	0.40	**0.72 (-)**	0.27	0.39	0.14	**0.69 (+)**
Gray Squirrel - Fall†	0.48	0.51	**0.84 (x)**	0.13	0.16	0.21	**0.83 (+)**
Gray Squirrel - Winter† ‡	0.23	0.47	0.24	**0.64 (q)**	0.17	0.20	0.23
Gray Squirrel - Spring†	0.38	0.42	**0.70 (x)**	0.15	0.15	0.20	**0.87 (+)**
Raccoon - Fall	0.14	0.33	0.45	0.16	0.48	0.35	**0.50 (+)**
Raccoon - Winter	0.28	0.36	0.18	**0.80 (-)**	0.18	0.47	**0.43 (+)**
Raccoon - Spring	0.10	0.19	0.26	0.27	**0.50 (-)**	0.22	0.19
Bear - Summer	0.17	0.25	0.47	0.19	0.20	0.20	**0.70 (-)**
Bear - Fall	0.22	0.25	**0.45 (+)**	0.22	**0.68 (+)**	0.23	0.17

† these models were run, where relevant, with an interaction effect between EDD and log. The sign of the coefficient is therefore not shown, but rather an ‘x’. See response curves in Figure 4 for more detail.

‡ camera height in this model selection process was included as a quadratic effect, and so the sign is not indicated next to the cumulative weight value, but rather a ‘q’. See Appendix S1: Figure S1 for more detail.

Table 4. Mean, standard deviation (SD), minimum and maximum raw detection probability (proportion of single-day occasions with a detection), and coefficient of variation (CV = SD/mean), recorded for five focal species for each of four seasons in a high-density camera grid with 27 camera stations. For comparison, values obtained from a previous study (SCBI Forest Grid), based on 29 (A) camera stations (1 station removed due to date/time recording errors) and 24 (B) at 500m grid separation are also shown. Fox squirrel were not modelled in this previous study.

Species and Season	Mean	SD	Min	Max	CV
White-tailed deer					
Summer	0.38	0.12	0.13	0.65	0.32
Fall	0.72	0.17	0.25	1.00	0.24
Winter	0.35	0.15	0.10	0.60	0.43
Spring	0.27	0.10	0.03	0.47	0.37
SCBI Forest Grid A	*0.32*	*0.23*	*0.04*	*0.83*	*0.71*
SCBI Forest Grid B	*0.26*	*0.17*	*0.00*	*0.64*	*0.67*
Fox squirrel (total)					
Summer	0.08	0.07	0.00	0.24	0.88
Fall	0.17	0.13	0.00	0.53	0.76
Winter	0.30	0.18	0.05	0.62	0.60
Spring	0.36	0.14	0.09	0.70	0.39
SCBI Forest Grid	*n/a*	*n/a*	*n/a*	*n/a*	*n/a*
Gray squirrel (total)					
Summer	0.05	0.05	0.00	0.16	1.00
Fall	0.09	0.12	0.00	0.38	1.33
Winter	0.12	0.12	0.00	0.42	1.00
Spring	0.32	0.13	0.10	0.59	0.41
SCBI Forest Grid A	*0.08*	*0.13*	*0.00*	*0.52*	*1.60*
SCBI Forest Grid B	*0.11*	*0.20*	*0.00*	*0.83*	*1.79*
Northern raccoon (total)					
Summer	0.03	0.04	0.00	0.18	1.33
Fall	0.12	0.09	0.00	0.35	0.75
Winter	0.24	0.16	0.04	0.67	0.67
Spring	0.10	0.06	0.03	0.24	0.60
SCBI Forest Grid A	*0.17*	*0.16*	*0.00*	*0.53*	*0.93*
SCBI Forest Grid B	*0.16*	*0.13*	*0.00*	*0.45*	*0.85*
Black bear (total)					
Summer	0.06	0.04	0.00	0.15	0.67
Fall	0.05	0.08	0.00	0.36	1.6
SCBI Forest Grid A	*0.06*	*0.09*	*0.00*	*0.40*	*1.40*
SCBI Forest Grid B	*0.07*	*0.07*	*0.00*	*0.27*	*1.08*

Table 5. Cumulative Model Weights for five covariates tested as covariates against probability of detection in single-season occupancy models with probability of occupancy held constant in each of 4 seasons for five focal species. Covariates include effective detection distance (EDD), camera height in cm (Height), dbh of oak trees in camera viewshed (Oak), total number of stems in camera viewshed (Stems) and the presence/absence of a log in the camera viewshed (Log). Those covariates selected in the top model are shown in bold and the sign of the coefficient (s) in the top models are indicated after each summed model weight. When no covariates are in bold, the intercept only model was the model with the lowest AICc value.

Species-Season	EDD	Height	Oak	Stems	Log
Deer – Summer	**0.50 (+)**	0.22	0.24	0.30	**1.00 (-)**
Deer – Fall	0.29	0.32	0.41	0.26	0.33
Deer – Winter	**0.63 (-)**	0.23	0.23	**0.62 (-)**	0.26
Deer – Spring	0.18	0.40	0.24	**0.82 (-)**	**0.79 (+)**
All Squirrel - Summer	**1.00 (-)**	**0.99 (-)**	0.00	0.00	**1.00 (+)**
All Squirrel - Fall† ‡	**1.00 (x)**	0.11	0.28	0.17	**1.00 (+)**
All Squirrel - Winter† ‡	**1.00 (x)**	0.00	0.01	**0.97 (+)**	**1.00 (+)**
All Squirrel - Spring† ‡	**0.98 (x)**	0.29	0.20	0.16	**1.00 (+)**
Fox Squirrel – Summer	**1.00 (-)**	**0.96 (-)**	0.02	0.02	**0.95 (+)**
Fox Squirrel – Fall	**1.00 (-)**	0.00	0.00	**1.00 (-)**	**1.00 (+)**
Fox Squirrel - Winter†	**1.00 (x)**	0.12	0.17	**0.40 (+)**	**1.00 (+)**
Fox Squirrel - Spring† ‡	**0.75 (+)**	**1.00 (q)**	0.25	0.18	0.25
Gray Squirrel – Summer	**0.95 (-)**	0.19	**0.40 (+)**	0.14	**0.99 (+)**
Gray Squirrel - Fall†	**1.00 (x)**	0.04	**0.80 (-)**	0.10	**1.00 (+)**
Gray Squirrel - Winter† ‡	**1.00 (x)**	**0.97 (q)**	0.01	0.02	**1.00 (+)**
Gray Squirrel - Spring† ‡	**1.00 (x)**	0.07	**0.67 (+)**	0.09	**1.00 (+)**
Raccoon – Summer	0.39	0.21	0.30	**1.00 (+)**	0.26
Raccoon – Fall	0.10	0.07	**0.93 (+)**	**0.98 (+)**	**0.78 (+)**
Raccoon – Winter	0.12	**1.00 (-)**	0.02	**1.00 (+)**	**0.83 (+)**
Raccoon – Spring	0.34	0.26	**0.80 (-)**	0.26	0.23
Bear – Summer	**0.52 (+)**	0.25	0.23	0.25	**0.81 (-)**
Bear – Fall	**0.95 (+)**	0.18	**0.98 (+)**	0.20	0.18

† these models were run, where relevant, with an interaction effect between EDD and log. The sign of the coefficient is therefore not shown, but rather an ‘x’. See Appendix S1: Figure S2 for more detail.

‡ camera height in this model selection process was included as a quadratic effect, and so the sign is not indicated next to the cumulative weight value, but rather a ‘q’. See Appendix S1: Figure S1 for more detail.

Figure legends

Figure 1. Mean capture rates (# of photo sequences/# days of deployment *100) for all species captured within a high-resolution camera grid of 27 cameras for 4 seasons. Error bars represent 95% confidence intervals. Inset figure displays magnified values for the 8 least commonly captured species.

Figure 2. Spatial patterns in capture rate variation across a 1-hectare sampling grid for 5 focal species in each of 4 sampling seasons, with point size reflecting capture rate (# of photo sequences/# days of deployment *100) values. Red asterisks indicate that the camera deployment failed entirely during that season. Values in the point size legends represent the median and first and third quartiles of capture rate for all cameras over all seasons. The point scale for the gray and fox squirrels are the same. Note that cameras were purposely offset from one row to the next.

Figure 3. Correlogram, truncated at 80m, for white-tailed deer capture rate values in summer (A), fall (B), winter (C), and spring (D) showing the relationship between inter-camera correlation value in capture rate, and inter-camera distance. A reference line at 20 m indicates the planned inter-camera distance and therefore a guide for the minimum inter-camera distance in the dataset on which to base inference.

Figure 4. Predicted count of sequences for combined squirrel species (fox, gray and unknown species) at different effective detection distances in Fall (A) and Spring (B) when a log was present (orange) or absent (blue) in the camera field of view. Predicted values are based on results of negative binomial generalized linear models, with an offset term for number of camera nights at each of 27 camera stations. In both cases the optimal model (shown here) included only log presence, effective detection distance, and their interaction. These same patterns were demonstrated (but not pictured) for gray squirrel models in Fall and Spring.

Figure 5. Spatial patterns in raw detection probability variation across a 1-hectare sampling grid for 5 focal species in each of 4 sampling seasons, with point size reflecting the proportion of single-day occasions resulting in a detection. Red asterisks indicate that the camera deployment failed entirely during that season.

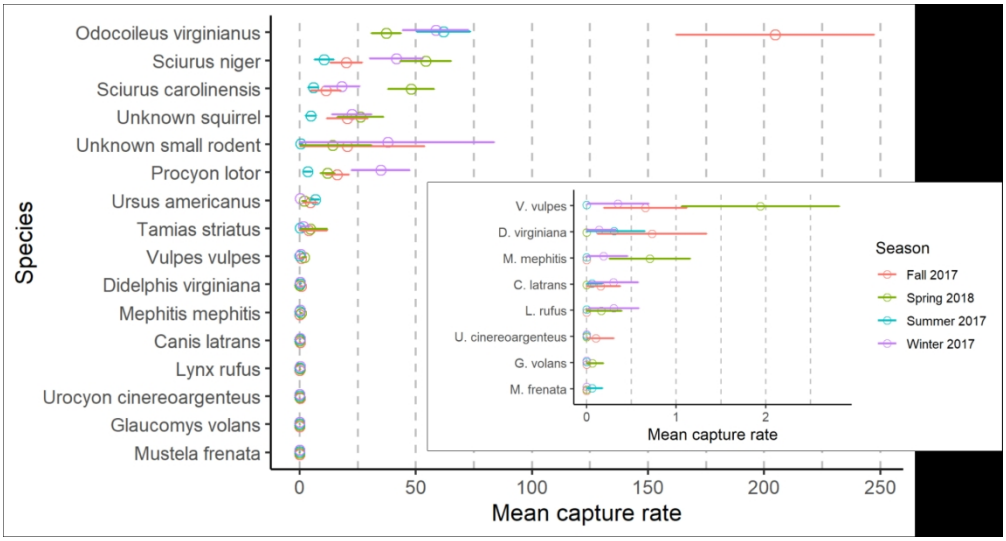

Figure 1. Mean capture rates (# of photo sequences/# days of deployment *100) for all species captured within a high-resolution camera grid of 27 cameras for 4 seasons. Error bars represent 95% confidence intervals. Inset figure displays magnified values for the 8 least commonly captured species.

216x115mm (240 x 240 DPI)

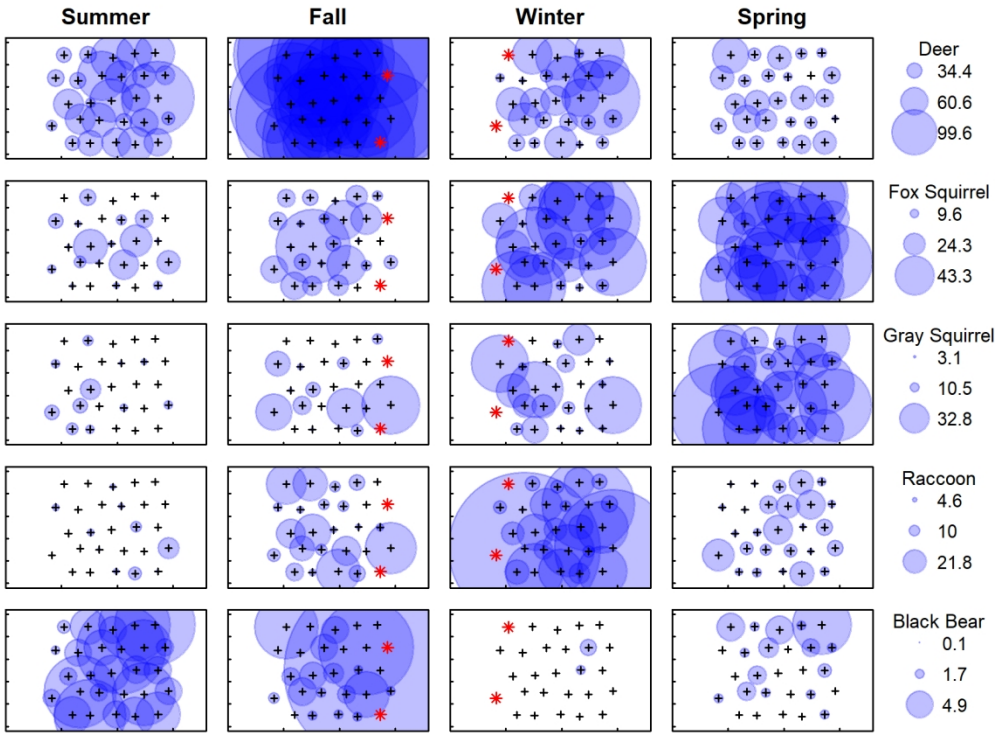

Figure 2. Spatial patterns in capture rate variation across a 1-hectare sampling grid for 5 focal species in each of 4 sampling seasons, with point size reflecting capture rate (# of photo sequences/# days of deployment *100) values. Red asterisks indicate that the camera deployment failed entirely during that season. Values in the point size legends represent the median and first and third quartiles of capture rate for all cameras over all seasons. The point scale for the gray and fox squirrels are the same. Note that cameras were purposely offset from one row to the next.

152x114mm (300 x 300 DPI)

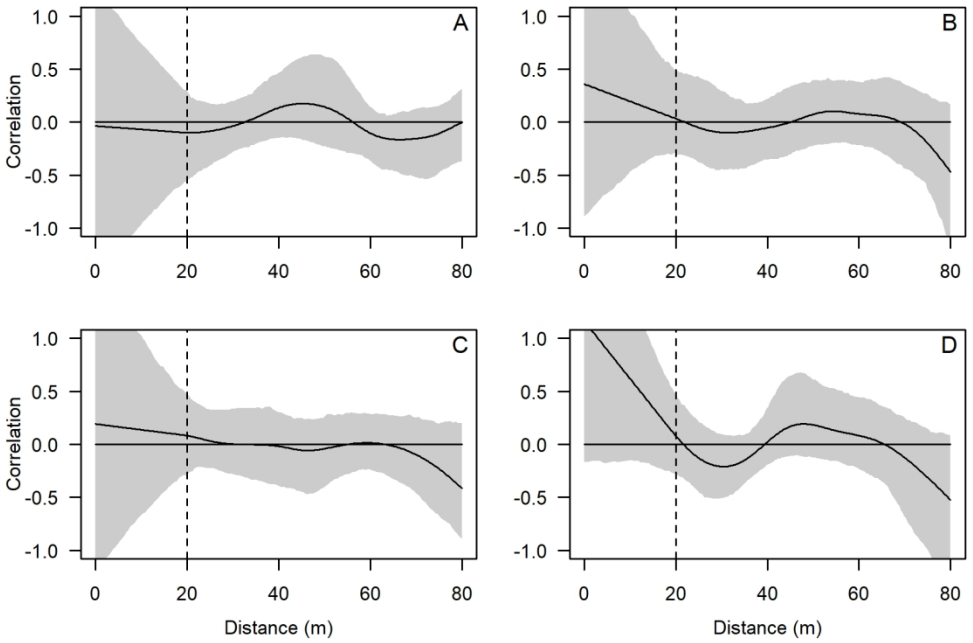

Figure 3. Correlogram, truncated at 80m, for white-tailed deer capture rate values in summer (A), fall (B), winter (C), and spring (D) showing the relationship between inter-camera correlation value in capture rate, and inter-camera distance. A reference line at 20 m indicates the planned inter-camera distance and therefore a guide for the minimum inter-camera distance in the dataset on which to base inference.

152x101mm (300 x 300 DPI)

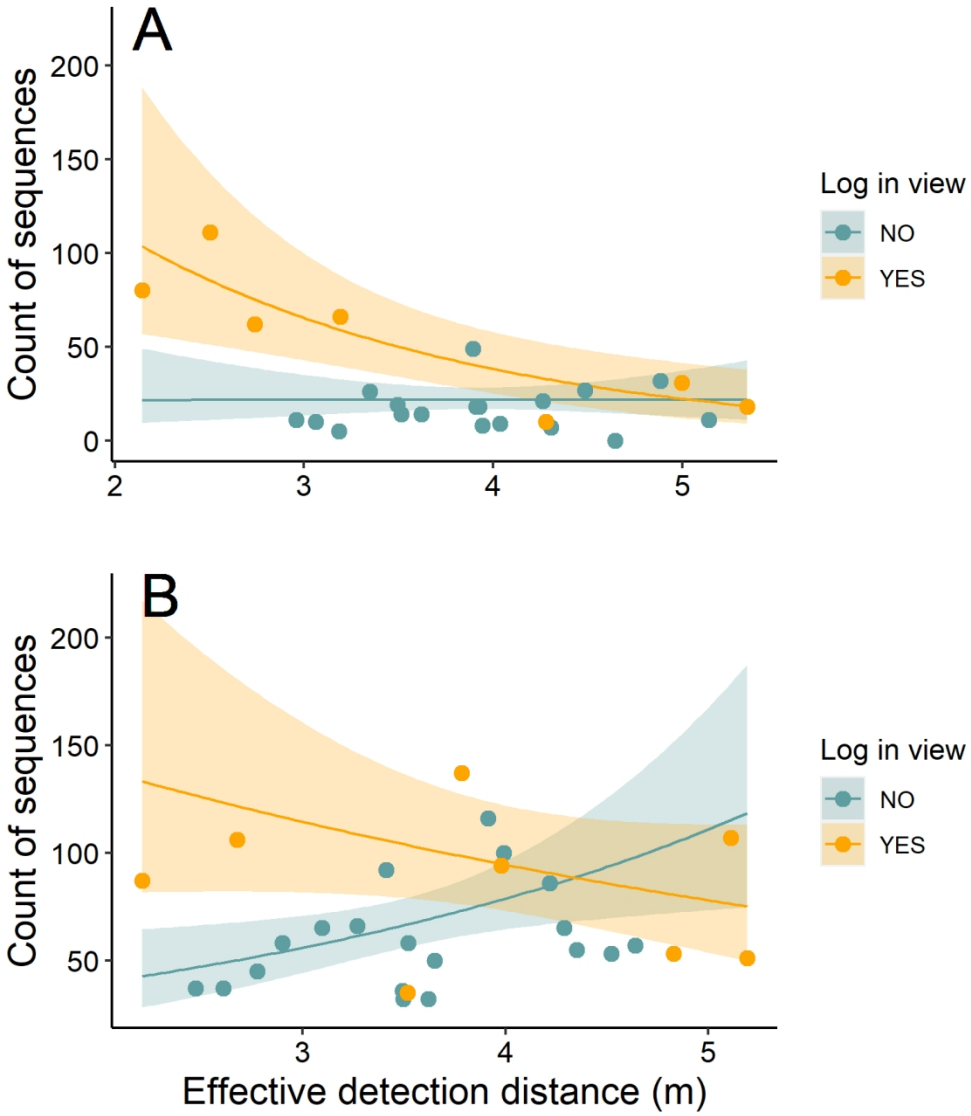

Figure 4. Predicted count of sequences for combined squirrel species (fox, gray and unknown species) at different effective detection distances in Fall (A) and Spring (B) when a log was present (orange) or absent (blue) in the camera field of view. Predicted values are based on results of negative binomial generalized linear models, with an offset term for number of camera nights at each of 27 camera stations. In both cases the optimal model (shown here) included only log presence, effective detection distance, and their interaction. These same patterns were demonstrated (but not pictured) for gray squirrel models in Fall and Spring.

134x152mm (300 x 300 DPI)

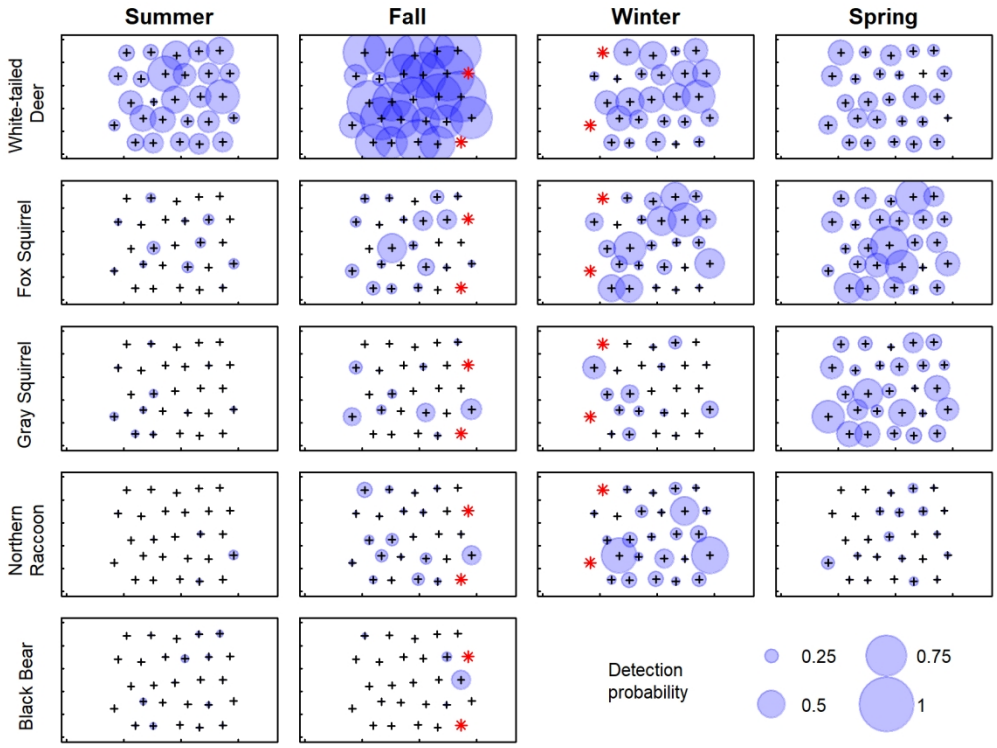

Figure 5. Spatial patterns in raw detection probability variation across a 1-hectare sampling grid for 5 focal species in each of 4 sampling seasons, with point size reflecting the proportion of single-day occasions resulting in a detection. Red asterisks indicate that the camera deployment failed entirely during that season.

152x114mm (300 x 300 DPI)